Pathology - Research and Practice 215 (2019) 152496

Contents lists available at ScienceDirect

Pathology - Research and Practice

journal homepage: www.elsevier.com/locate/prp

A fetal mouse model of ventricular non-compaction using retinoic acid

Cao Fei[a], Yang Zhenglin[a], Yin Lixue[a,b,*]

[a] School of Medicine, University of Electronic Science and Technology of China, Chengdu 610054, China
[b] Sichuan Provincial Key Laboratory for Ultrasound in Cardiac Electrophysiology and Biomechanics, Sichuan Provincial People's Hospital, University of Electronic Science and Technology of China, Chengdu 610072, China

ARTICLE INFO

Keywords:
Animal model
Retinoic acid (RA)
Non-Compaction of ventricular myocardium (NVM)

ABSTRACT

Objective: To develop a fetal mouse model of non-compaction of ventricular myocardium (NVM) using All-trans retinoic acid (ATRA).

Methods: Pregnant mice were divided into blank control group, dimethyl sulfoxide (DMSO) control group and ATRA group. The pregnant mice at 8.5 days after pregnancy were given 70 mg/kg ATRA in DMSO to induce fetal mouse model of NVM in ATRA group. All the hearts were acquired and sliced in short axis from the neonatal mice sacrificed after delivery. Pathological changes were visualized under 40- and 100-fold magnification with Hematoxylin-eosin (HE) staining at different ventricular levels. The criteria for pathological diagnosis of classical NVM were: prominent trabeculations on the endocardial surface and deep intertrabecular recesses communicating with the ventricular cavity and the thickness ratio of non-compacted layer (N) to compact myocardium layer (C) N/C > 1.4. Analysis of variance (ANOVA) and least significant difference (LSD) were used to analyze the differences of three groups, with $P < 0.05$ considered as significant.

Results: The typical characteristics of NVM histopathological findings of ATRA fetal mouse were confirmed: compared to the hearts of blank control group (n = 20) and DMSO control group (n = 15), all the hearts of ATRA group (n = 17) showed the obviously thinner compacted layer and the much thicker non-compacted layer. The N/C ratio of left ventricles (LVs) in ATRA group was 2.735 ± 1.634, higher than those in DMSO control group 0.178 ± 0.119 and blank control group 0.195 ± 0.118 with significant difference ($F = 32.550$, $P < 0.0001$); N/C ratios of right ventricles (RVs) in the ATRA group were (6.068 ± 4.394), higher than those in the DMSO control group 0.459 ± 0.24 and in the blank control group 0.248 ± 0.182 with significant difference ($F = 20.069$, $P < 0.0001$). LSD of LVs and RVs showed a significant difference between ATRA and blank control group ($P < 0.0001$), and between ATRA and DMSO control group ($P < 0.0001$). LSD showed no significant difference in two control groups of LVs ($P = 0.963$) and of RVs ($P = 0.848$) .

Conclusion: Excess ATRA could be used to induce NVM of fetal mice heart. This animal model might provide a platform for fundamental research of NVM pathogenesis and potential targeting treatment.

1. Introduction

Non-compaction of ventricular myocardium (NVM), known as 'spongy myocardium', is a rare type of cardiac syndrome. It is characterized by a pattern of prominent trabeculations on the endocardial surface and deep intertrabecular recesses communicating with the ventricular cavity [1]. It has been postulated that NVM is a malfunction of embryonic heart development, caused by intrauterine developmental arrest of the normal myocardial compaction process during the first trimester of pregnancy. Consequently, the segmental spongy myocardium fails to transform into compaction and leads to a formation of two layers of the ventricular myocardium: the compacted layer and the non-compacted layer [2,3]. During normal development, the compacting process of the left ventricular myocardium comes later than that of the right ventricle, so the NVM lesion mostly occurs in the left ventricle (LV) and mainly involves the apex of the heart [4–6].

Prevalence of NVM in the adult population ranges between 0.01% and 0.27% according to echocardiography studies [7]. Recent reports suggest that NVM is a genetically heterogeneous disorder, which may constitute up to 9% of childhood cardiomyopathies and is becoming the third most common cardiomyopathy among pediatric patients [8,9]. Major complications of NVM include heart failure (HF), arrhythmias, systemic thromboembolic events, and sudden cardiac death. The diagnostic modalities of NVM include, but are not limited to, echocardiography and magnetic resonance imaging (MRI). By far, two-dimensional echocardiography (2DE) is the most commonly used diagnostic

* Corresponding author.
E-mail address: yinlixue_cardiac@163.com (L. Yin).

https://doi.org/10.1016/j.prp.2019.152496
Received 3 April 2019; Received in revised form 26 May 2019; Accepted 8 June 2019

modality [10]. There is no specific treatment or reversal of disease progression for NVM, and its management depends on the recognition of different clinical manifestations [11]. Long-term prognosis for patients with NVM depends on the stage and progression of heart failure, the occurrence of thromboembolic events, and the different types of arrhythmias [12]. A much better prognosis has been noted in patients with fewer involved LV segments than in those with more [13]. Other research publications also reported that the severity of non-compaction in a given segment is more important than the number of involved segments for prognosis in humans [14].Findings from genetically engineered mouse NVM models suggest that defects in myofibrillogenesis and polarization in trabecular cardiomyocytes underlie ventricular non-compaction pathogenesis [9]. Overexpression of mutations in α-dystrobrevin (*DTNA*) in the mouse heart results in a phenotype similar to left ventricular non-compaction (LVNC), which leads to deep trabeculation, dilated cardiomyopathy, and cardiac dysfunction [15].

Retinoic acid (RA) is an active derivative of vitamin A, which has an essential role in normal cardiac development [16]. In offspring of vitamin A-deficient mothers, the myocardium of the ventricular walls was thinner and walls were less compact than in hearts from control fetuses of the same age [17]. Many of the cardiovascular anomalies in rats with vitamin A deficiency closely resemble malformations observed in humans [17,18].

RA deficiency or overdose can interfere in its signal transduction pathway resulting in abnormal communication between the cardiac neural crest cells (CNCCs) and the second heart field (SHF) cells, which postpones the addition of progenitor cells from SHF to the poles of the elongating cardiac tube and cardiac artery and then leads to various congenital cardiac malformations with predominance of outflow tract (OFT) defects [19–21].

NVM is a life-threatening cardiac syndrome, and it is usually considered to be a genetic heart disease. The progressive non-compaction changes of the left ventricular wall are often accompanied by systolic dysfunction, and there is a positive correlation between the extent of non-compaction and the degree of systolic dysfunction [22]. So far, there are no effective methods of treatment due to its unclear etiology and pathogenesis. Therefore, an effective NVM experimental animal model is particularly important for investigating the pathogenesis and for acquiring a better understanding of the mechanism of myocardial development and construction, which would facilitate targeted treatment of NVM. In this study we hypothesized that an overdose of RA applied during the embryonic stage of ventricular architecture development, specifically during cardiac tube elongation and looping, induces non-compaction of the ventricular myocardium. Here, we introduce a BALB/c mouse model of NVM to enable further exploration of NVM pathogenesis.

2. Materials and methods

2.1. Reagents

ATRA (Cat. No. R2625, Sigma, St Louis, Mo, USA) was dissolved in dimethylsulfoxide (DMSO, D2438-50ML Sigma) at the final concentration of 35 mg/ml. All procedures with ATRA were performed under dimmed light to prevent photo-damage of the compound. About 40 mg RA can dissolve in 1 ml DMSO. In our experiments, we found almost all the pregnant mice were dead if each mouse was injected with 4 ml/kg DMSO, but if the dose reduced to 2 ml/kg, all the mice can live well, so we use 2 mg/kg DMSO to dissolve ATRA powder in ATRA group. We designed corresponding DMSO without ATRA as control group. We also did a lot of preliminary experiments to optimize the concentration of ATRA. In the preliminary experiments, 80 mg/kg, 70 mg/kg, 60 mg/kg, 40 mg/kg and 20 mg/kg ATRA were dissolved into 2 ml DMSO respectively. We found 70 mg/kg is the optimized ATRA concentration that can induce the classical NVM pathology of fetal mouse without being lethal of pregnant mice.

2.2. Preparation of mouse models of NVM

Healthy C57BL/6 mice (16-week-old inbred strains, 20–30 g) for the experiment were purchased from the Institute of Laboratory Animals of Sichuan Provincial People's Hospital &. Sichuan Academy of Medical Sciences (certificate No. SYXK 2013-110).

Adult female and male mice were mated 2:1 and pregnancy was confirmed for pregnancy by checking the vaginal plug in females. Pregnant mice were randomly divided into 3 groups, such that the final count of analyzed offspring samples was 40. 1. In the blank control group (n = 15), neonatal mice were sacrificed immediately after birth; 2. In the DMSO control group (n = 12), pregnant mice were given DMSO by intraperitoneal injection (2 ml/kg) at 8.5 days post coitus (dpc); 3. In the ATRA group (n = 13), ATRA (70 mg/kg) dissolved in 2 ml DMSO was intraperitoneally administered to pregnant mice at 8.5 dpc. All mice were kept in the experimental animal room, which was maintained according to standard husbandry procedures in individually ventilated cages (IVC) of an air-conditioned room at temperatures ranging 20–26 °C. They were fed a normal diet and given water. All experimental procedures involving animals were performed in strict accordance with the guidelines approved by the Ethics Committee of the School of Medicine, University of Electronic Science and Technology of China.

2.3. Tissue collection and histopathological staining

All the hearts of three groups were acquired for about 20 (18–21) dpc from the neonatal mice who were sacrificed immediately after normal delivery of pregnant mice to match some neonatal mice in the ATRA group who suffered from severe NVM and died soon after the birth. The hearts collected from neonatal mice were fixed in 4% paraformaldehyde in phosphate buffered saline (PBS) for 48 h, dehydrated and then embedded in paraffin. One slice from each heart was chosen for measurement perpendicular to the long axis from: 1. the apical section; 2. the middle section between the apex and the base of the heart (midventricular level); or 3. from the basal level below the forming atrioventricular valves (subvalvular level). Slices were then embedded in paraffin blocks. Sections (4 μm thick) were dewaxed, rehydrated, and then stained with Hematoxylin-eosin.

2.4. Imaging

Offspring heart sections were visualized and their images captured at 40X and 100X magnification using the NIKON ECLIPSE CI optical microscope, equipped with a NIKON DS-U3 imaging system (Nikon, Japan) for visual inspection of the thickness of the compacted layer and non-compacted layer (trabeculated myocardium).

Clinically, NVM diagnosis relies on Doppler echocardiography. In adults, the threshold ratio of non-compacted myocardium (N) to compact myocardium (C) at the end of the systole is considered to be to 2.0, such that an N/C > 2.0 signifies NVM [23]. In children, this ratio threshold is set at 1.4 [24]. However, there is no equivalent diagnostic criterion for "non-compacted myocardium" in mice. The evaluation criteria for a successful NVM model are instead: a pattern of prominent trabeculations on the endocardial surface and deep intertrabecular recesses communicating with the ventricular cavity. N/C > 1.4 is now used as the diagnostic criterion for myocardial densification insufficiency in neonatal mice.

2.5. Statistical analysis

To determine N/C ratios, we measured the classical LV lesion of each slice for the distance between the trabecular recess and trabecular tip (N) and between the epicardium and the trabecular recess (C), as shown in Fig. 4. Significant differences in N/C ratios among the three groups were tested by one-way ANOVA. Adjustment for multiple

comparisons between groups was done by LSD test in analysis of variance. A $P < 0.05$ was considered as the threshold for statistical significance.

3. Results

3.1. Behavioral characteristics of mice and their off-spring

During the study, pregnant mice in the ATRA or DMSO group were in good condition and had no significant behavioral abnormalities. The daily food and water intake, mental state, activity, as well as stool and urine volume were normal. During pregnancy and childbirth, the fertility rates of the blank control group and the DMSO group were normal, and there was no significant difference between the two groups. In the ATRA group, birth rates were reduced due to premature birth, dystocia, and embryonic and fetal death. The yield and productivity of pregnant mice in the ATRA intervention group was about 10% lower than the control group and the DMSO group. There was no significant difference in the productivity or birth rate of pregnant mice between the control group and the DMSO group.

3.2. Histopathological changes of cardiac tissues in NVM mouse models

Paraffin sections and HE staining showed that 100% of mouse offspring (17/17) in the ATRA group had spongy changes in the left ventricular myocardium. Although the size of the heart displayed no obvious changes (Figs. 1–3), the diameter of some chambers was noticeably smaller (Figs. 1–2) or larger (Fig. 3). In the 100X images of trabecular muscles at the site of lesion in this group, we can see that the space between the trabecular muscles was deeper, wider, and filled with blood, and the density of myocardial cells was lower, but the arrangement of endothelial cells on the endocardium was still regular. Furthermore, all mice in the ATRA group met the diagnostic criteria of $N/C > 1.4$. In the DMSO control and the blank control group, there were almost no obvious changes in myocardial compaction. The N/C ratios were measured in the ATRA group (17 mice including LV n = 3, RV n = 4, LV and RV n = 10), the DMSO control group (15 mice including LV N = 3, RV n = 3, LV and RV n = 9) and the blank control group (20 mice including LV n = 8, RV n = 5, LV n = and RV n = 7), respectively. The results of Tables 1–3 were as follows: N/C ratios of left ventricles in the ATRA group (n = 13) were (2.735 ± 1.634), in the DMSO control group (n = 12) (0.178 ± 0.119) and in the blank control group (n = 15) (0.195 ± 0.118). One-way ANOVA revealed that there was a significant difference among the three groups ($F = 32.550$, $P < 0.0001$). Multiple comparisons of LSD analysis of variance between groups showed a significant difference between the ATRA group and the blank control group, $P < 0.0001$. The ATRA group and the DMSO control group was $P < 0.0001$; There was no significant difference between the DMSO control group and blank control group ($P = 0.963$). N/C ratios of right ventricles in the ATRA group (n = 14) were (6.068 ± 4.394), in the DMSO control group (n = 12) (0.459 ± 0.24) and in the blank control group (n = 12) (0.248 ± 0.182). One-way ANOVA revealed that there was a significant difference among the three groups ($F = 20.069$, $P < 0.0001$). Multiple comparisons of LSD analysis of variance between groups showed a significant difference between the ATRA group and the blank control group, $P < 0.0001$. The ATRA group and the DMSO control group was $P < 0.0001$; There was no significant difference between the DMSO control group and blank control group ($P = 0.848$).

Histopathology demonstrated that the two layers of the myocardium – epicardial compacted layer and subendocardial non-compacted layer – differed markedly in the ATRA group from the two control groups. Compared to the blank control and DMSO control groups, the heart slices of the ATRA group had a thin epicardial compacted layer and a thick subendocardial non-compacted layer with numerous, excessively prominent trabeculations, including deep trabeculations in the ventricular wall that define recesses communicating with the main ventricular chamber, as shown in Figs. 1–3. Additionally, the subendocardial myocardial structure was disordered compared to the control hearts. This pattern of prominent trabeculations on the endocardial surface and deep intertrabecular recesses communicating with the ventricular cavity as well as the loss of compaction in structure represent classical morphological NVM characteristics.

Furthermore, we observed differences in ventricular morphology of the ATRA group. 1. Near the apex of the LV, the non-compacted layer is significantly thicker and the compacted layer is obviously thinner (Fig. 1e,f) compared to the blank control (Fig. 1a,b) and the DMSO control (Fig. 1c,d). 2. Near the mitral valve plane of the short axis, heart slices have a visibly thicker non-compacted layer (N) and thinner compacted layer (C) in both ventricles (Fig. 2g–i) compared to the blank control (Fig. 2a–c) and the DMSO control (Fig. 2d–f) groups. 3. In Fig. 3, heart slices also from the mitral valve plane of the short axis show a remarkably thinner compacted layer in both ventricles in the ATRA group (3e,f) compared to the blank control (Fig. 3a,b) and the DMSO control (Fig. 3c,d), and the non-compaction of the RV is more severe than that of the LV in the ATRA group (Fig. 3e,f).

4. Discussion

The main histopathological feature of NVM is myocardial malformation characterized by the presence of subendocardial myocardial layer with numerous prominent trabeculations and deep inter-trabecular recesses [25]. This discovery as well as advances in medical diagnostic procedures continues to improve the accuracy of NVM diagnoses. A retrospective epidemiological study of childhood cardiomyopathy in Australia analyzed all cases of primary cardiomyopathy in children under 10 years of age who presented between 1987 and 1996. Over the 10-year period, 314 new cases of primary cardiomyopathy were identified, and left ventricular non-compaction explained 9.2 percent of cases, which is second only to dilated cardiomyopathy and hypertrophic cardiomyopathy [26].

However, the exact etiology of NVM is currently still speculative. Given that the majority of documented cases are congenital, the prevailing theory is that the normal process of myocardial compaction is arrested during embryonic development, resulting in an excess of immature trabeculated myocardium [27]. Although many different gene mutations have been reported in patients with NVM, such as *G4.5 (TAZ), DTNA, ZASP, ACTC, TNNT2* and *MYH7* [28], the concrete cause and underlying pathological mechanism are very complex and remain largely unknown.

RA plays a crucial role in the formation of the compact myocardial layer of the ventricular wall during myocardial development. Normal ventricular myocardial compaction depends on the proper amount of RA, secreted by retinoid-producing EPDCs [29]. RA is synthesized by retinaldehyde dehydrogenase 2 (RALDH2), an enzyme found in epicardial-derived epithelial cells (EPDCs), during and after the heart looping stage of embryonic development. These cells release RA into the developing ventricular muscular layers in the embryo. The main sites of RA-responsive elements are present in SHF cells and in CNCCs where they contribute to the development of the heart [30]. Activated by RA, SHF cells promote elongation of the cardiac tube poles and outflow tract (OFT) development. This takes place while multipotent progenitor cells differentiate into myocardium, smooth muscle, and endothelial cells [31].

Relevant findings about a thinned or poorly developed myocardial wall in some of the offspring of RA-deficient rats have been reported in an early study by Wilson and Warkany [19]. Non-compaction of the ventricular myocardium has been confirmed in *Raldh2* knock-out mice, unable to produce the RALDH2 enzyme [32,33]. Since RALDH2 is the major enzyme for retinoic acid synthesis during embryonic development, these *Raldh2* knock-out mice can be considered RA-deficient

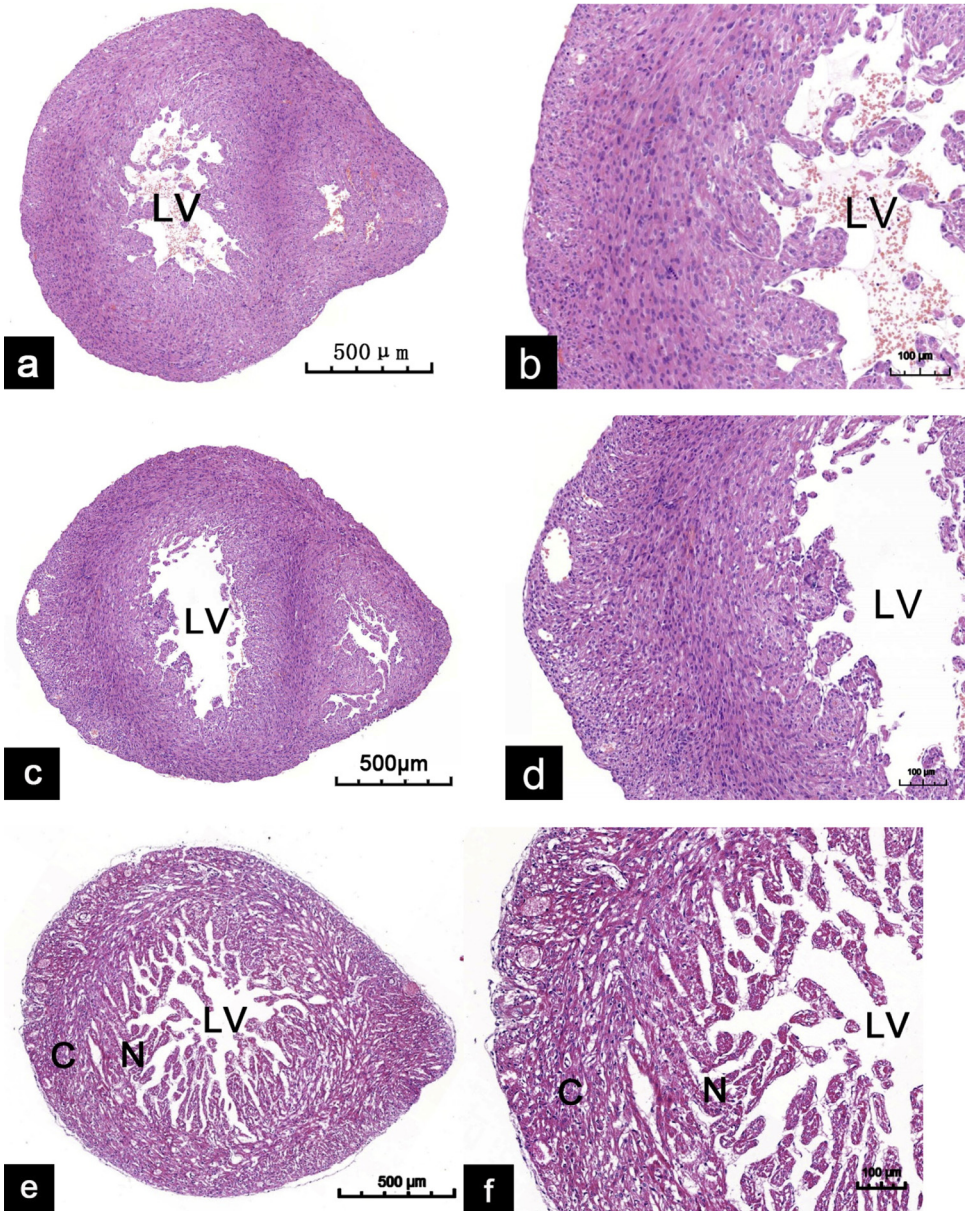

Fig. 1. Displayed here are representative histological sections of the apical region of LV taken from each group at 40X (a,c,e) and 100X (b,d,f) magnifications. (a,b are blank control; c,d are DMSO control; e,f are ATRA). Sections of the heart were in the apical region of the LV cut perpendicularly to the long axis starting from the apex. HE staining of e, f sections shows a severely thickened, 2-layered myocardium: the prominently thinner compacted layer (corresponding to letter C) and the significantly thicker non-compacted layer (corresponding to letter N). Numerous prominent trabeculations and deep intertrabecular recesses are visible in the inner surface of the non-compacted layer (N) in the apical region of LV (e,f), which is much thicker than in the blank control heart (a,b) and DMSO control heart (c,d). LV — left ventricle; C— compacted layer; N— non-compacted layer.

[34]. Therefore, RA deficiency during embryogenesis in pregnant mice causes non-compaction cardiomyopathy in their offspring.

Given that a specific amount of RA is required to promote myocardial maturation and form a normal compacted ventricular myocardial wall for cardiac development during embryogenesis, RA is likely to be involved in signal transduction pathways that are important for building the proper compact myocardium. Thus, an overdose of RA may cause a thick endocardial layer of prominent trabeculations and thin epicardial layer of the compact myocardial wall, similar to that in RA deficiency.

Review of recent scientific literature substantiates our use of the RA overdose to induce NVM onset. The CNCCs play a critical role in the pathogenesis of various human cardiocraniofacial syndromes such as CHARGE, Noonan syndromes and Retinoic Acid Embryopathy. RA as a ligand is an essential upstream regulator of CNCCs that binds RA receptors (RARs) and retinoid X receptors (RXRs) in these cells and is involved in various molecular signaling pathways of heart development during the embryonic stage [35]. RA reduces signaling in the fibroblast growth factor 8 (FGF8) pathway within the SHF by down-regulating insulin gene enhancer protein (ISL1) to control heart anteroposterior patterning [36]. RA also activates downstream genes Hoxa1 and Hoxa3 of the Hox family, which are expressed in distinct sub-domains of the SHF and in cardiac progenitor cells that contribute to both atria and the inferior wall of the OFT [37]. The importance of retinoid signaling during cardiac development has long been appreciated but recently has become a rapidly expanding field of research. It is evident that intact and controlled retinoid signaling is necessary for each stage of cardiac development to proceed normally, including cardiac lineage determination, heart tube formation, looping, epicardium formation, ventricular maturation, chamber and outflow tract septation, and coronary arteriogenesis [38].

Wnt/β-catenin-independent signaling encompasses several different pathways, of which the most extensively studied is the planar cell polarity (PCP) pathway responsible for planar polarization of cell structures within an epithelial sheet. During cardiac development, RA activates the Wnt/beta-catenin signaling pathway by Wnt ligand binding to downstream receptors, such as Frizzed (FZD), Dishevelled (DVL), or Vang, and then regulates several differentiation and proliferation processes of cardiac progenitor myocytes. The PCP pathway controls a variety of cell behaviors such as polarized protrusive cell activity,

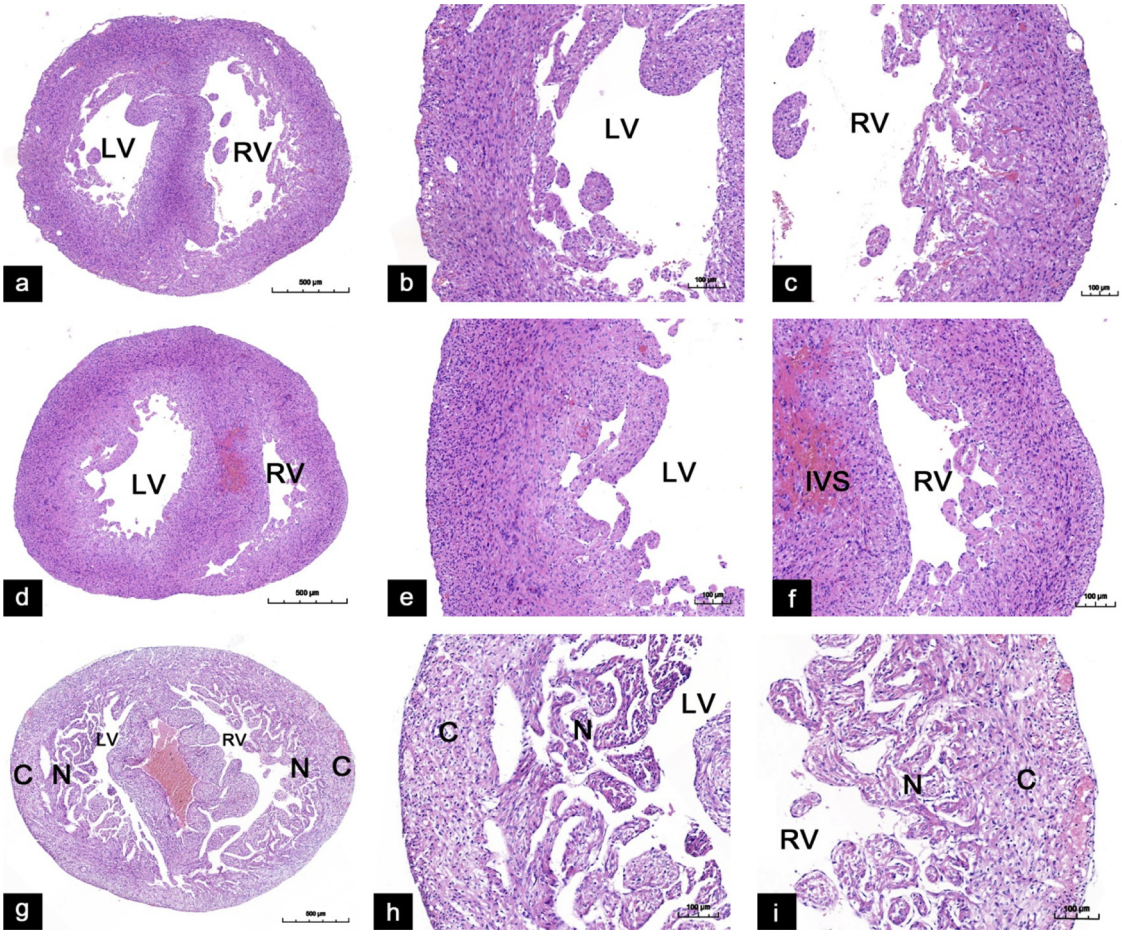

Fig. 2. Displayed here are representative histological sections of the two ventricles (LV and RV) taken from each group at 40X (a,d,g) and 100X (b,c,e,f,h,i) magnifications. (a,b,c are blank control; d,e,f are DMSO control; g,h,i are ATRA). Heart slices were near the mitral valve plane of the short axis cut perpendicularly to the long axis from the apex. HE staining of g,h,i sections shows a 2-layered myocardium: the thinner compacted layer (marked "C") and the thicker non-compacted layer (marked "N"). Numerous prominent trabeculations and deep intertrabecular recesses are visible in the inner surface of the non-compacted layer (N) in both ventricles of the ATRA heart (g,h,i). The compacted layer is obviously thinner than in the blank control heart (a,b,c) and DMSO control heart (d,e,f). The ATRA heart also displays disordered subendocardial myocardial structure in the non-compacted layer compared to the two control groups. RV — right ventricle; IVS — interventricular septum.

directional cell movement, and oriented cell division [38–42]. Cardiomyocytes cannot be polarized and maintain round shape if the normal PCP pathway is disturbed, which leads to non-compaction of myocardium [39]· An RA overdose might interfere with the proper PCP pathway of cardiomyocyte development and induce the non-compaction of myocardium.The aim of our study was to build a mouse model of NVM in mouse offspring by administering to pregnant mice a teratogenic dose of RA. This hypothesis is borne out by our study's findings, which show that an overdose of RA causes myocardial wall underdevelopment and leads to a non-compacted structure of the ventricular wall. Given that previously reported ATRA dosage of the most potent teratogenic effect without being lethal was 70–80 mg/kg body weight in mice [43–45], in our study, we administered ATRA at 70 mg/kg b.w. (body weight). Non-compaction myocardium in our experimental mouse model confirmed by pathomorphological examination presented as a thick endocardial layer of numerous, excessively prominent trabeculations and a thin epicardial compact layer of the myocardial wall in RA-treated mouse offspring (Figs. 1–3), which are classical NVM histopathological characteristics.

In some hearts of the ATRA-interfered group, we observed that non-compaction in themyocardial wall of the RV was more severe than that of the LV (Fig. 3). Since SHF cells are highly sensitive to RA signaling and contribute markedly to the development of the RV and both inflow and outflow poles [46,47], it is generally recognized that without the addition of SHF cells to the elongating heart tube during cardiac development the outflow tract is shortened and can develop malformations [48]. The thinning of the RV compacted myocardial wall may be caused by abnormal migration of SHF cells to the heart tube.

Since NVM is a rare cardiac condition in humans, reports of NVM incidence in humans have been limited to case studies. The pathogenesis of some cases with a known family history has been traced to gene mutations such as *G4.5* (Tafazzin, *TAZ*), *DTNA* gene related to myocardial development [28]. There are also idiopathic cases with insufficient clinical epidemiological data. Whether family history is known or not, case reports do not provide complete information about mothers' exposure during pregnancy to potential environmental risk factors at different stages of foetal development, although one study is an exception [49]. Nevertheless, we cannot rule out the possibility that excessive RA might contribute to the development of non-compaction myocardium and outflow tract malformations in human embryos during pregnancy [49,50].

Additional observations from our study are: 1. the development of ventricular non-compaction in the earliest stage that could be confirmed by histomorphological examination of the myocardial wall took place after birth; 2. the non-compaction in these mouse models was visible in the LV (3 mice), in the RV (4 mice), or both ventricles (10 mice), and also in the interventricular septum; 3. in some hearts, the non-compaction layer involved the whole myocardial wall and in others

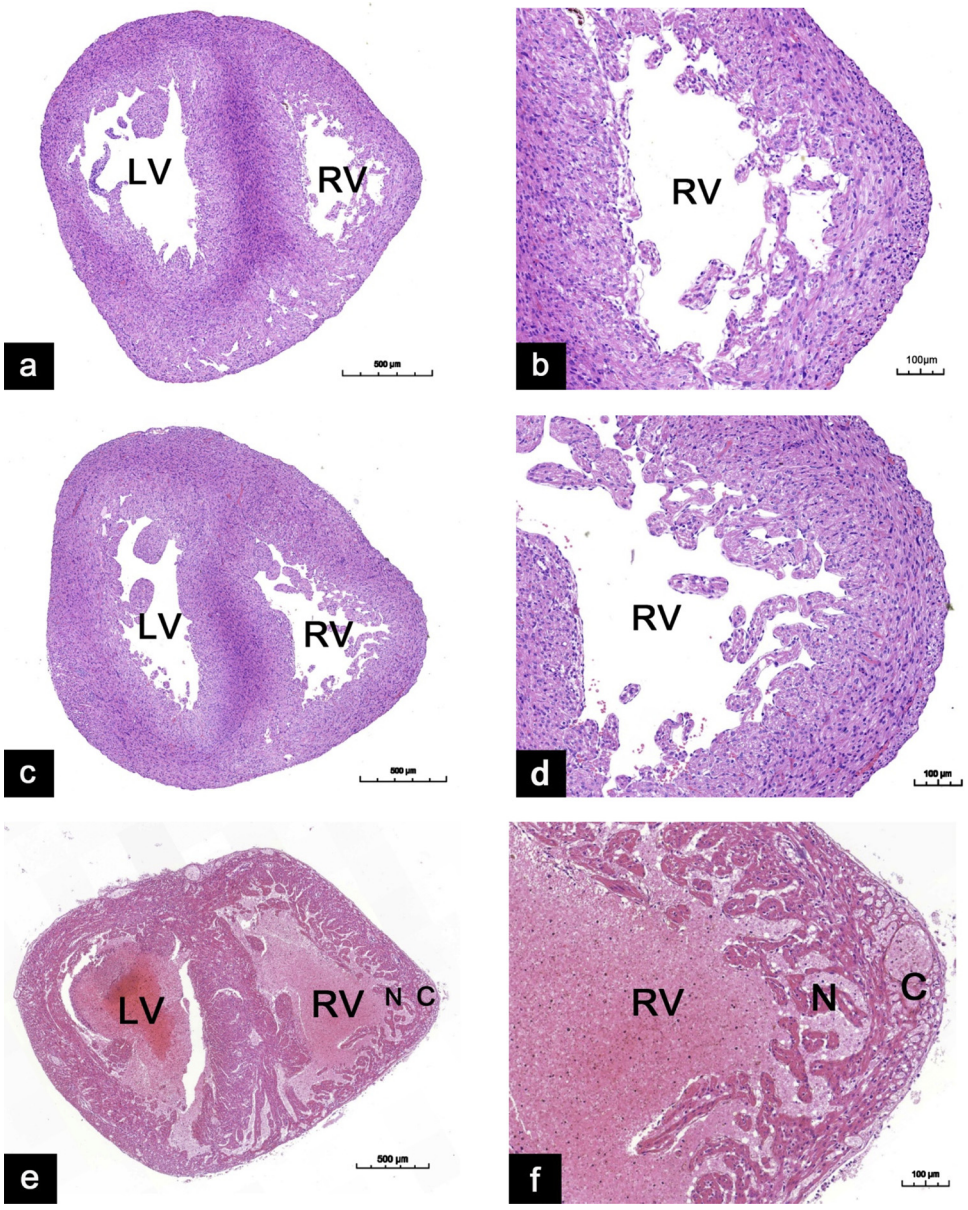

Fig. 3. Displayed here are representative histological sections of right ventricles (RV) taken from each group at 40X (a,c,e) and 100X (b,d,f) magnifications. (a,b are blank control; c,d are DMSO control; e,f are ATRA). Heart slices were at the mitral valve plane of the short axis cut perpendicularly to the long axis from the apex. HE staining of e, f sections shows 2-layered myocardium: the obviously thinner compacted layer (corresponding to letter C) and the non-compacted layer (corresponding to letter N). In ATRA group occurs remarkably thinner compacted layer of both ventricles compared to the blank control (Figure a,b) and the DMSO control (Figure c,d), in which non-compaction of the RV was more severe than that of the LV in ATRA group (Figure e,f).

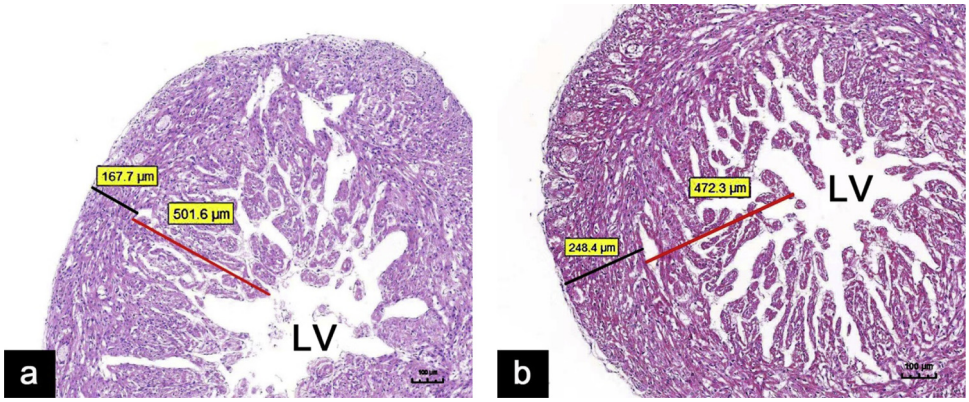

Fig. 4. Displayed here are measurements of distance between the trabecular recess and trabecular tip (non-compacted (N), red line) and between the epicardium and trabecular recess (compact (C), black line) on cardiac slices (Figure a,b). Magnification: a. 100X; b. 100 X.

Table 1
The measurement value of non-compacted myocardium layer (N) and compact myocardium layer (C) and the value of N/C ratio of the left ventricles in blank control group (n = 15), DMSO control group (n = 12) and ATRA group (n = 13).

	Control group						ATRA group			P value (N/C)
	Blank control group			DMSO control group						
	N(μm)	C(μm)	N/C	N(μm)	C(μm)	N/C	N(μm)	C(μm)	N/C	
	66.6	348	0.191	137.2	384.9	0.356	580	74.6	7.775	
	0	571.5	0	33.2	328.6	0.101	525.5	244	2.154	
	122.9	482.7	0.255	26.2	337.5	0.078	279.9	81.3	3.443	
	35.5	345.7	0.103	67.4	369.1	0.183	238.4	166.3	1.434	
	83.3	346.8	0.240	119.9	326.1	0.368	702.4	205	3.426	
	113.6	411.6	0.276	86.3	383.4	0.225	496.1	244.2	2.032	
	151	393.6	0.384	53.8	328.6	0.164	458.4	244.3	1.876	
	112.6	495.4	0.227	97.7	408	0.239	411.9	169.7	2.427	
	79.8	367.8	0.217	0	373.8	0	501.6	167.8	2.989	
	119.1	419.4	0.284	0	390.9	0	417.4	196.6	2.123	
	108.7	383.2	0.284	107.6	475.4	0.226	542.3	294.4	1.842	
	58.2	305.3	0.191	66.9	340.6	0.196	472.3	248.4	1.901	
	104.8	383.4	0.273				589.6	275.9	2.137	
	0	396	0							
	0	453.3	0							
M ± SD	77.1 ± 49.1	406.9 ± 69.2	0.195 ± 0.118	66.4 ± 45.4	370.6 ± 43.4	0.178 ± 0.119	478.1 ± 124.4	201.0 ± 68.2	2.735 ± 1.634	p < 0.0001

N- The thickness of non-compacted myocardium layer; C- The thickness of compact myocardium layer. The mean values (M) of the value of N, C and N/C ratio with standard deviation (M ± SD). One-way ANOVA and multiple comparisons with SPSS 22.0 statistical software was used to analyze N/C ratio among the three groups. A p value below 0.05 proved to be statistically significant.

it was seen only in one segment of only one ventricle. Since the RA overdose was directly involved in the metabolism of fetal mice during pregnancy, the study approximates well human congenital, naturally occurring NVM. Given that RA is administered to the mouse foetuses, the model we propose allows RA to interfere with their *in utero* metabolism as well as disrupt DNA transcription and translation downstream of RA binding, as would be expected to happen in human congenital NVM. Changes in transcriptional and translational levels of downstream pathway mediators could, in turn, answer important questions for the prevention and treatment of NVM.

The model we propose can be used as a reference of NVM pathological features to improve the accuracy of diagnosis and avoid misdiagnosis. Giving timely clinical treatment can reduce the mortality of NVM patients. Additionally, by providing an animal NVM model, we hope this study will facilitate the exploration of novel treatment options. Lastly, additional research may identify novel connections between RA and NVM, which may further improve diagnosis and treatment of NVM. Given that NVM frequently occurs in conjunction with one or more congenital cardiac anomalies, including ventricular septal defects, atrial septal defects, valvular abnormalities, coarctation of the aorta and anomalous pulmonary veins [51,52], in future studies we plan to observe other cardiovascular abnormalities in addition to non-compaction myocardium. Additionally, we plan to examine molecular changes within the relevant pathway at the transcriptional and translational level after administrating RA.

Limitations of this study include a small sample size and unknown translatability to other species.

Table 2
The measurement value of non-compacted myocardium layer (N) and compact myocardium layer (C) and the value of N/C ratio of the right ventricles in blank control group (n = 12), DMSO control group (n = 12) and ATRA group (n = 14).

	Control group						ATRA group			P value (N/C)
	Blank control group			DMSO control group						
	N(μm)	C(μm)	N/C	N(μm)	C(μm)	N/C	N(μm)	C(μm)	N/C	
	29	206.8	0.140	78.2	456.4	0.171	619.5	39.8	15.565	
	63.2	330.8	0.191	80.6	233.1	0.346	151.7	14.7	10.320	
	189.4	269.7	0.702	53.1	218	0.244	259.3	76.4	3.394	
	98.2	320.1	0.307	135.1	262.8	0.514	475.5	60.7	7.834	
	59	164.3	0.359	161.2	250.5	0.644	301.3	144.5	2.085	
	55.3	252.2	0.219	169.5	260.9	0.650	375	143	2.622	
	83.1	268.1	0.310	140.7	358.1	0.393	338.6	73.6	4.601	
	61.4	232.2	0.264	168.4	291.2	0.578	457	36.8	12.418	
	0	190.7	0.000	222.9	255.9	0.871	412.3	254.8	1.618	
	0	284.1	0.000	182.8	305.9	0.598	216	88.4	2.443	
	63.5	253.6	0.250	0	334.4	0.000	507.1	151.1	3.356	
	64.8	277.7	0.233	122	243.6	0.501	503.5	206.1	2.443	
							414.2	48.5	8.540	
							375.6	48.7	7.713	
M ± SD	63.9 ± 49.3	254.2 ± 49.5	0.248 ± 0.182	126.2 ± 62.8	289.2 ± 67.0	0.459 ± 0.24	386.2 ± 126.2	99.1 ± 70.6	6.068 ± 4.394	p < 0.0001

N- The thickness of non-compacted myocardium layer; C- The thickness of compact myocardium layer. The mean values (M) of the value of N, C and N/C ratio with standard deviation (M ± SD). One-way ANOVA and multiple comparisons with SPSS 22.0 statistical software was used to analyze N/C ratio among the three groups. A p value below 0.05 proved to be statistically significant.

Table 3
The results of one-way ANOVA and multiple comparisons of N/C ratio with SPSS 22.0 statistical software in left and right ventricles among the blank control group, DMSO control group and ATRA group.

			Significance (p value)	
			Left ventricle	Right ventricle
One-way ANOVA	Blank control group, DMSO control group and ATRA group		.000	.000
Multiple comparisons	Blank control group	DMSO control group	.963	.848
	ATRA group	Blank control group	.000	.000
	ATRA group	DMSO control group	.000	.000

A p value below 0.05 proved to be statistically significant. One-way ANOVA of N/C ratio showed: F = 32.550 in left ventricle and F = 20.069 in right ventricle.

5. Conclusions

Here we introduce a fetal mouse model of NVM induced by administering excess ATRA to pregnant mice at the stage of embryonic heart tube elongation and looping. It is the hope of our research group that this animal model may serve as a platform for fundamental studies of NVM pathogenesis and potential targeting treatment.

Acknowledgements

The research funding was provided by National Natural Science Foundation of ChinaNo. 81671852

References

[1] S. Uribe, L. Cadavid, T. Hussain, et al., Cardiovascular magnetic resonance findings in a pediatric population with isolated left ventricular non-compaction, J. Cardiovasc. Magn. Reson. 14 (2012) 9, https://doi.org/10.1186/1532-429X-14-9.
[2] K. Reynen, K. Bachmann, H. Singer, Spongy myocardium, Cardiology 88 (6) (1997) 601–602, https://doi.org/10.1159/000177433.
[3] M.M. Benjamin, R.A. Khetan, R.C. Kowal, et al., Diagnosis of left ventricular non-compaction by computed tomography, Proc. Bayl. Univ. Med. Cent. 25 (4) (2012) 354–356.
[4] C. Stollberger, J. Finsterer, G. Blazek, Left ventricular hypertrabeculation/non-compaction and association with additional cardiac abnormalities and neuromuscular disorders, Am. J. Cardiol. 90 (8) (2002) 899–902.
[5] D. Sedmera, T. McQuinn, Embryogenesis of the heart muscle, Heart Fail. Clin. 4 (3) (2008) 235–245, https://doi.org/10.1016/j.hfc.2008.02.007.
[6] G. Minardi, C. Manzara, G. Pulignano, et al., Adult bi-ventricular noncompaction cardiomyopathy, Anadolu Kardiyol. Derg. 10 (2) (2010) 188–190, https://doi.org/10.5152/akd.2010.049.
[7] T.K. Chin, J.K. Perloff, R.G. Williams, et al., Isolated noncompaction of left ventricular myocardium. A study of eight cases, Circulation 82 (2) (1990) 507–513.
[8] D.U. Udeoji, K.J. Philip, R.P. Morrissey, et al., Left ventricular noncompaction cardiomyopathy: updated review, Ther. Adv. Cardiovasc. Dis. 7 (5) (2013) 260–273, https://doi.org/10.1177/1753944713504639.
[9] Y. Liu, H. Chen, W. Shou, Potential common pathogenic pathways for the left ventricular noncompaction cardiomyopathy (LVNC), Pediatr. Cardiol. 39 (6) (2018) 1099–1106, https://doi.org/10.1007/s00246-018-1882-z.
[10] B.C. Weiford, V.D. Subbarao, K.M. Mulhern, Noncompaction of the ventricular myocardium, Circulation 109 (24) (2004) 2965–2971, https://doi.org/10.1161/01.CIR.0000132478.60674.D0.
[11] Z.Z. Song, Echocardiography in the diagnosis left ventricular noncompaction, Cardiovasc. Ultrasound 6 (2008) 64, https://doi.org/10.1186/1476-7120-6-64.
[12] U. Ikeda, M. Minamisawa, J. Koyama, Isolated left ventricular non-compaction cardiomyopathy in adults, J. Cardiol. 65 (2) (2015) 91–97, https://doi.org/10.1016/j.jjcc.2014.10.005.
[13] K. Papadopoulos, P.M. Petrou, D. Michaelides, Left ventricular noncompaction cardiomyopathy presenting with heart failure in a 35-Year-Old man, Tex. Heart Inst. J. 44 (4) (2017) 260–263, https://doi.org/10.14503/THIJ-15-5371.
[14] C. Cevik, R.F. Stainback, Isolated left ventricular noncompaction in a 90-year-old man, Tex. Heart Inst. J. 39 (2) (2012) 255–257.
[15] Q. Cao, Y. Shen, X. Liu, et al., Phenotype and functional analyses in a transgenic mouse model of left ventricular noncompaction caused by a DTNA mutation, Int. Heart J. 58 (6) (2017) 939–947, https://doi.org/10.1536/ihj.16-019.
[16] A. Canete, E. Cano, R. Munoz-Chapuli, et al., Role of vitamin A/Retinoic acid in regulation of embryonic and adult hematopoiesis, Nutrients 9 (2) (2017), https://doi.org/10.3390/nu9020159.
[17] R.K. Kam, Y. Deng, Y. Chen, et al., Retinoic acid synthesis and functions in early embryonic development, Cell Biosci. 2 (1) (2012) 11, https://doi.org/10.1186/2045-3701-2-11.
[18] S.A. Ross, P.J. McCaffery, U.C. Drager, et al., Retinoids in embryonal development, Physiol. Rev. 80 (3) (2000) 1021–1054, https://doi.org/10.1152/physrev.2000.80.3.1021.
[19] J.G. Wilson, J. Warkany, Aortic-arch and cardiac anomalies in the offspring of vitamin A deficient rats, Am. J. Anat. 85 (1) (1949) 113–155.
[20] J.G. Wilson, J. Warkany, Cardiac and aortic arch anomalies in the offspring of vitamin A deficient rats correlated with similar human anomalies, Pediatrics 5 (4) (1950) 708–725.
[21] A. Kolodzinska, A. Heleniak, A. Ratajska, Retinoic acid-induced ventricular non-compacted cardiomyopathy in mice, Kardiol. Pol. 71 (5) (2013) 447–452, https://doi.org/10.5603/KP.2013.0090.
[22] I.M. Hutchins, S. Schaefer, Progressive left ventricular noncompaction and systolic dysfunction, Exp. Clin. Cardiol. 17 (2) (2012) 81–83.
[23] R. Jenni, E. Oechslin, J. Schneider, et al., Echocardiographic and pathoanatomical characteristics of isolated left ventricular non-compaction: a step towards classification as a distinct cardiomyopathy, Heart 86 (6) (2001) 666–671, https://doi.org/10.1136/heart.86.6.666.
[24] R.H. Pignatelli, C.J. McMahon, W.J. Dreyer, et al., Clinical characterization of left ventricular noncompaction in children: a relatively common form of cardiomyopathy, Circulation 108 (21) (2003) 2672–2678, https://doi.org/10.1161/01.CIR.0000100664.10777.B8.
[25] O. Mirea, M. Berceanu, A. Constantin, et al., Non-compaction cardiomyopathy – brief review. 4 (2) (2017) 115–124.
[26] A.W. Nugent, P.E. Daubeney, P. Chondros, et al., The epidemiology of childhood cardiomyopathy in Australia, N. Engl. J. Med. 348 (17) (2003) 1639–1646, https://doi.org/10.1056/NEJMoa021737.
[27] G. Captur, P. Nihoyannopoulos, Left ventricular non-compaction: genetic heterogeneity, diagnosis and clinical course, Int. J. Cardiol. 140 (2) (2010) 145–153, https://doi.org/10.1016/j.ijcard.2009.07.003.
[28] S. Klaassen, S. Probst, E. Oechslin, et al., Mutations in sarcomere protein genes in left ventricular noncompaction, Circulation 117 (22) (2008) 2893–2901, https://doi.org/10.1161/CIRCULATIONAHA.107.746164.
[29] J.M. Perez-Pomares, A. Phelps, M. Sedmerova, et al., Experimental studies on the spatiotemporal expression of WT1 and RALDH2 in the embryonic avian heart: a model for the regulation of myocardial and valvuloseptal development by epicardially derived cells (EPDCs), Dev. Biol. (Basel) 247 (2) (2002) 307–326.
[30] P. Dolle, V. Fraulob, J. Gallego-Llamas, et al., Fate of retinoic acid-activated embryonic cell lineages, Dev. Dyn. 239 (12) (2010) 3260–3274, https://doi.org/10.1002/dvdy.22479.
[31] R.G. Kelly, The second heart field, Curr. Top. Dev. Biol. 100 (2012) 33–65, https://doi.org/10.1016/B978-0-12-387786-4.00002-6.
[32] K. Niederreither, J. Vermot, N. Messaddeq, et al., Embryonic retinoic acid synthesis is essential for heart morphogenesis in the mouse, Development 128 (7) (2001) 1019–1031.
[33] S.C. Lin, P. Dolle, L. Ryckebusch, et al., Endogenous retinoic acid regulates cardiac progenitor differentiation, Proc Natl Acad Sci U S A 107 (20) (2010) 9234–9239, https://doi.org/10.1073/pnas.0910430107.
[34] M. Theodosiou, V. Laudet, M. Schubert, From carrot to clinic: an overview of the retinoic acid signaling pathway, Cell. Mol. Life Sci. 67 (9) (2010) 1423–1445, https://doi.org/10.1007/s00018-010-0268-z.
[35] A. Keyte, M.R. Hutson, The neural crest in cardiac congenital anomalies, Differentiation 84 (1) (2012) 25–40, https://doi.org/10.1016/j.diff.2012.04.005.
[36] I.O. Sirbu, X. Zhao, G. Duester, Retinoic acid controls heart anteroposterior patterning by down-regulating Isl1 through the Fgf8 pathway, Dev. Dyn. 237 (6) (2008) 1627–1635, https://doi.org/10.1002/dvdy.21570.
[37] N. Bertrand, M. Roux, L. Ryckebüsch, et al., Hox genes define distinct progenitor sub-domains within the second heart field, Dev. Biol. 353 (2) (2011) 266.
[38] L.L. Hoover, E.G. Burton, B.A. Brooks, et al., The expanding role for retinoid signaling in heart development, ScientificWorldJournal 8 (2008) 194–211, https://doi.org/10.1100/tsw.2008.39.
[39] D.J. Henderson, R.H. Anderson, The development and structure of the ventricles in the human heart, Pediatr. Cardiol. 30 (5) (2009) 588–596, https://doi.org/10.1007/s00246-009-9390-9.
[40] S. Babayeva, B. Rocque, L. Aoudjit, et al., Planar cell polarity pathway regulates nephrin endocytosis in developing podocytes, J. Biol. Chem. 288 (33) (2013) 24035–24048, https://doi.org/10.1074/jbc.M113.452904.
[41] C.D. Fraser Jr., Evolution of the pediatric and congenital heart surgery service at Texas Children's Hospital: 1954-2015, Semin. Thorac. Cardiovasc. Surg. 27 (4) (2015) 380–387, https://doi.org/10.1053/j.semtcvs.2015.11.003.
[42] M. Almuedo-Castillo, E. Saló, T. Adell, Dishevelled is essential for neural connectivity and planar cell polarity in planarians, Proceedings of the National Academy of Sciences 108 (7) (2011) 2813–2818, https://doi.org/10.1073/pnas.1012090108.

[43] B.A. Fraser, A.A. Travill, The effect of retinoic acid on chondrogenesis in the fetal hamster tibia in vivo, J. Embryol. Exp. Morphol. 48 (1978) 23–35.
[44] H. Wang, W. Chen, Dose-dependent antiteratogenic effects of folic acid on all-trans retinoic acid-induced cleft palate in fetal mice, Cleft Palate Craniofac. J. 53 (6) (2016) 720–726, https://doi.org/10.1597/15-170.
[45] H. Yasui, M. Nakazawa, M. Morishima, et al., Morphological observations on the pathogenetic process of transposition of the great arteries induced by retinoic acid in mice, Circulation 91 (9) (1995) 2478–2486.
[46] L. Ryckebusch, Z. Wang, N. Bertrand, et al., Retinoic acid deficiency alters second heart field formation, Proc Natl Acad Sci U S A 105 (8) (2008) 2913–2918, https://doi.org/10.1073/pnas.0712344105.
[47] M. Buckingham, S. Meilhac, S. Zaffran, Building the mammalian heart from two sources of myocardial cells, Nat. Rev. Genet. 6 (11) (2005) 826–835, https://doi.org/10.1038/nrg1710.
[48] T.M. Yelbuz, K.L. Waldo, D.H. Kumiski, et al., Shortened outflow tract leads to altered cardiac looping after neural crest ablation, Circulation 106 (4) (2002) 504–510.
[49] K.J. Jenkins, A. Correa, J.A. Feinstein, et al., Noninherited risk factors and congenital cardiovascular defects: current knowledge: a scientific statement from the American Heart Association Council on Cardiovascular Disease in the Young: endorsed by the American Academy of Pediatrics, Circulation 115 (23) (2007) 2995–3014, https://doi.org/10.1161/CIRCULATIONAHA.106.183216.
[50] E.J. Lammer, D.T. Chen, R.M. Hoar, et al., Retinoic acid embryopathy, N. Engl. J. Med. 313 (14) (1985) 837–841, https://doi.org/10.1056/NEJM198510033131401.
[51] G. Fazio, S. Pipitone, M.A. Iacona, et al., The noncompaction of the left ventricular myocardium: our paediatric experience, J. Cardiovasc. Med. Hagerstown (Hagerstown) 8 (11) (2007) 904–908, https://doi.org/10.2459/JCM.0b013e32801462b0.
[52] A. Burke, E. Mont, R. Kutys, et al., Left ventricular noncompaction: a pathological study of 14 cases, Hum. Pathol. 36 (4) (2005) 403–411, https://doi.org/10.1016/j.humpath.2005.02.004.